

## Modulation of UK lightning by heliospheric magnetic field polarity

This content has been downloaded from IOPscience. Please scroll down to see the full text.

2014 Environ. Res. Lett. 9 115009

(<http://iopscience.iop.org/1748-9326/9/11/115009>)

View [the table of contents for this issue](#), or go to the [journal homepage](#) for more

Download details:

IP Address: 82.5.40.96

This content was downloaded on 19/11/2014 at 06:51

Please note that [terms and conditions apply](#).

# Modulation of UK lightning by heliospheric magnetic field polarity

M J Owens<sup>1</sup>, C J Scott<sup>1</sup>, M Lockwood<sup>1</sup>, L Barnard<sup>1</sup>, R G Harrison<sup>1</sup>, K Nicoll<sup>1</sup>, C Watt<sup>1</sup> and A J Bennett<sup>2</sup>

<sup>1</sup>Department of Meteorology, University of Reading, UK

<sup>2</sup>Bristol Industrial and Research Associates Limited, Bristol, UK

E-mail: [m.j.owens@reading.ac.uk](mailto:m.j.owens@reading.ac.uk)

Received 22 September 2014, revised 24 October 2014

Accepted for publication 24 October 2014

Published 18 November 2014

## Abstract

Observational studies have reported solar magnetic modulation of terrestrial lightning on a range of time scales, from days to decades. The proposed mechanism is two-step: lightning rates vary with galactic cosmic ray (GCR) flux incident on Earth, either via changes in atmospheric conductivity and/or direct triggering of lightning. GCR flux is, in turn, primarily controlled by the heliospheric magnetic field (HMF) intensity. Consequently, global changes in lightning rates are expected. This study instead considers HMF polarity, which doesn't greatly affect total GCR flux. Opposing HMF polarities are, however, associated with a 40–60% difference in observed UK lightning and thunder rates. As HMF polarity skews the terrestrial magnetosphere from its nominal position, this perturbs local ionospheric potential at high latitudes and local exposure to energetic charged particles from the magnetosphere. We speculate as to the mechanism(s) by which this may, in turn, redistribute the global location and/or intensity of thunderstorm activity.


Keywords: lightning, thunderstorm, solar wind, heliospheric magnetic field, atmospheric electric circuit

## 1. Introduction

The electrification of thunderclouds is generally accepted to result from strong updrafts in the mixed-phase region (e.g., [4]), where the presence of both a downward flux of graupel and an upward flux of ice crystals can produce charge transfer and separation by collisions [24]. Indeed, parameterization of these processes [8] in numerical weather prediction models has led to successful forecasts of lightning flash rates [30]. A number of observational studies, however, suggest lightning flash rates may also be modulated to some degree by external factors such as solar magnetic activity [25], though the mechanism(s) and even sign of response are still under debate. On solar-cycle timescales, both positive [27] and negative [21] correlations have been found between sunspot number and thunderstorm activity. On shorter time scales, lightning over the USA has been found to decrease

following impulsive reductions in galactic cosmic ray (GCR) flux by strong heliospheric magnetic field (HMF) enhancements [6]. Conversely, smaller, recurrent HMF structures appear to increase UK lightning and thunder rates, possibly via lower energy solar particles compensating for the GCR decrease [26]. These thunderstorm trends have all been linked with changes in energetic charged particle flux incident on Earth and hence changes in global atmospheric conductivity [9] and/or global lightning trigger rates [22].

The HMF is formed by the solar wind dragging coronal magnetic loops anti-sunward while both magnetic foot points remain rooted on the rotating solar surface [19]. Thus the large-scale HMF forms an Archimedean spiral, making an angle of approximately 45° to the Earth–Sun line in near-Earth space. If the overall polarity of the HMF is pointing toward (*T*) the Sun, near-Earth HMF will have magnetic field components  $B_X > 0$  and  $B_Y < 0$  in geocentric solar ecliptic coordinates (where *X* points towards the Sun, *Y* points away from Earth's orbital motion and *Z* is normal to the ecliptic plane), whereas away polarity (*A*) will result in  $B_X < 0$  and  $B_Y > 0$ . At any one instant, there are typically 2 or 4 large-

 Content from this work may be used under the terms of the Creative Commons Attribution 3.0 licence. Any further distribution of this work must maintain attribution to the author(s) and the title of the work, journal citation and DOI.

scale  $T$  or  $A$  ‘sectors’ in Earth’s orbital plane, meaning the Earth is embedded in a given sector for an average of 7–14 days (e.g., [18]). This study investigates the effect of HMF polarity on lightning occurrence.

## 2. Data

There are a number of methods for detecting thunderstorm activity, but long-term studies at mid-to-high geomagnetic latitudes are best performed by radio networks, which detect radio sferics from lightning strokes. In this study, lightning stroke rates,  $R_L$ , were obtained from the UK Met Office’s arrival time difference (ATD) network of radio receivers in Western Europe [15]. It detects the VLF component of broadband emission (‘sferics’) from lightning and uses the relative timing to determine location. The ATD system is primarily sensitive to cloud-to-ground (CG) lightning over Europe, but can detect lightning worldwide with reduced sensitivity. In order to ensure uniformity of the lightning measurements and enable more direct comparison with the UK-based thunder-day data described below, lightning data are limited to events within a radius of 500 km of central England. Ongoing development of lightning detection systems makes long-term thunderstorm activity studies problematic. However, between September 2000 and May 2005 the ATD system was not subject to any modifications affecting its sensitivity. After this period the radio network was expanded and increased in sensitivity to form ATDnet, which detects a larger number of smaller sferics. During May 2005 to 2007, this increase was only moderate, with the annual mean of  $R_L$  increasing by around 50%. We include these data in the study by normalizing  $R_L$  after May 2005 by 0.64, though accept that this results in the inclusion of smaller lightning events than in the initial period. (We note that our results are largely unchanged whether these later data are included or not.) Post May 2007, further developments to ATDnet meant the sensitivity increased by around 400%. Without any means to discriminate between CG lightning and smaller, inter-cloud lightning, these data are dominated by qualitatively different lightning events from pre-2007. In order to not preferentially emphasize any one season, we only consider whole years of data, 2001 through 2006 inclusive. Data are converted to daily mean lightning stroke rates to remove any diurnal variations and to enable direct comparison with  $R_{TH}$  data.

Audible thunder records from UK Met Office manned observing sites can serve as an independent, if low fidelity, validation of radio observations. This observation is subject to false positives (such as vehicle noise or explosions) and is of a lower time resolution compared with the ATD lightning data, but crucially its detection efficiency is not subject to the ionospheric effects which could potentially affect  $R_L$ . We compute a ‘thunder day rate’,  $R_{TH}$ , defined as the fraction of UK manned stations which reported thunder on a given day. Any stations which did not report a single instance of thunder in a given year were assumed to not be logging such information and excluded from the study. Note that  $R_{TH}$  will be affected by the mean altitude, and hence audibility, of

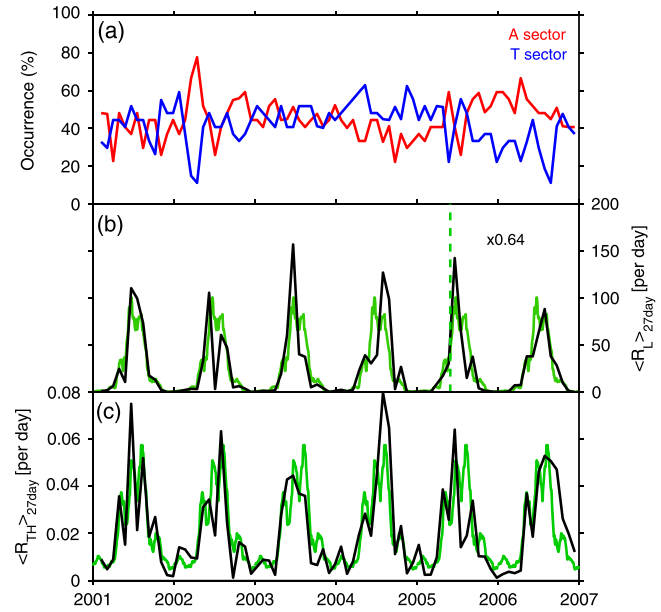


**Figure 1.** Time series of the datasets used in this study. (a) The percentage occurrence of away ( $A$ , red) and toward ( $T$ , blue) heliospheric magnetic field sectors. (b)  $R_L$ , the daily UK lightning stroke rate from the ATD radio network (black) and its mean seasonal variation (green). (c)  $R_{TH}$ , UK thunder day rate (black) and its mean seasonal variation (green). All data have been 27 day averaged for purposes of plot clarity, but all analysis in this study is performed on daily data.

thunderstorms over the UK and thus may be sensitive to somewhat different forms/intensities of thunderstorm activity than  $R_L$ .

Figures 1(b) and (c) show the  $R_L$  and  $R_{TH}$  time series, respectively, further averaged to 27 day means for clarity (all analysis, however, is performed on daily means). As expected, there is general agreement between these two thunderstorm measurements, particularly in the seasonal trends. We find linear correlations in daily data of  $r = 0.573$  (sample size,  $N$ , of 2134) and 27 day mean data of  $r = 0.817$  ( $N = 80$ ). These correlations and sample sizes result in ‘ $p$ -values’ of effectively zero, meaning the null hypothesis (that the correlation occurred by chance) can be rejected at almost 100% confidence, as one would expect. On the other hand, perfect correlation (i.e.,  $r = 1$ ) should not be expected, as the dynamic ranges of the two time series are vastly different (e.g., thunder days, as a binary measure, will measure the same value for days with 1 or 1000 lightning flashes). Furthermore,  $R_L$  and  $R_{TH}$  may be sensitive to slightly different properties and/or magnitudes of thunderstorm activity.

Heliospheric magnetic sector structure is determined using hourly OMNI data [12], which collates various near-Earth spacecraft measurements and propagates them to the nose of the magnetosphere. Simple daily means of  $B_X$  and  $B_Y$  can be heavily skewed by short ‘spikes’ in field magnitude and could therefore be unrepresentative of the resulting large-scale ionospheric potential patterns, which generally vary over longer timescales. Instead, each hour of data is flagged as 1 if  $B_Y > 0$  and  $B_X < 0$ ,  $-1$  if  $B_Y < 0$  and  $B_X > 0$ , or 0 if neither set of criteria are met. Daily  $A$  ( $T$ ) sectors are intervals

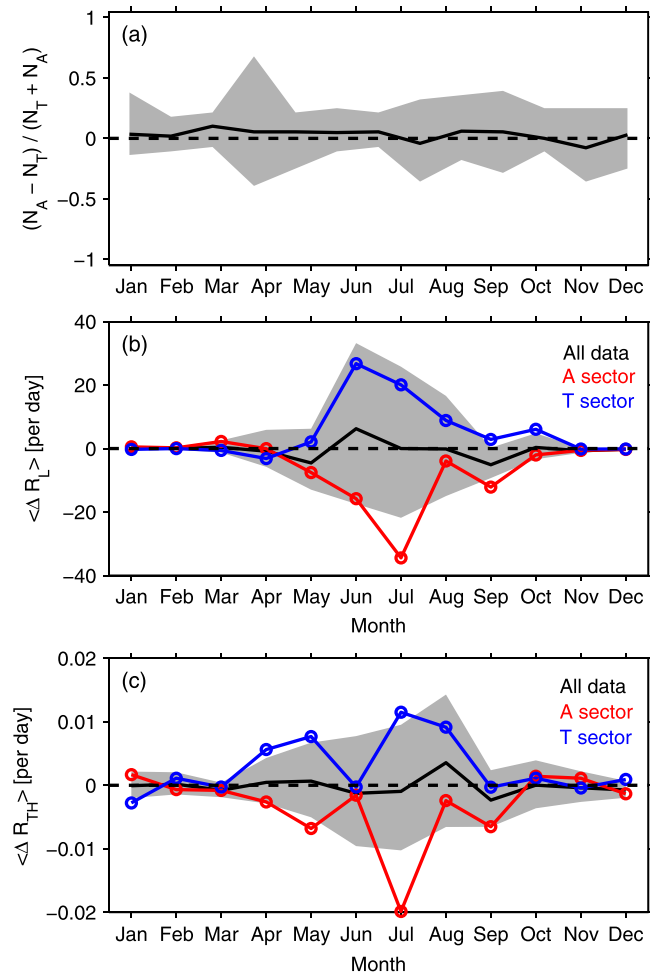


**Figure 2.** Monthly means of (a) the fractional occurrence of toward (*T*) and away (*A*) heliospheric magnetic field sectors, with the grey-shaded area showing the maximum and minimum occurrence in any individual year, (b) UK lightning rates relative to the seasonal mean,  $\Delta R_L$ , for all data (black), *A* (red) and *T* (blue) sectors and (c) UK thunder day rates relative to the seasonal mean,  $\Delta R_{TH}$ , in the same format as (b). Grey shaded areas in (b) and (c) show 90% of the variations over the whole dataset.

in which the 24 hour mean is  $> 0.3 (< -0.3)$ . Figure 1(a) shows the percentage occurrence rate of *T* and *A* days per solar rotation (approximately 27 days). The period 2001 through 2006 exhibits relatively small annual trends (figure 1(a)) and almost no seasonal trend (figure 2(a)) in sector occurrence, reducing the likelihood of systematic aliasing between sector occurrence and thunderstorm activity. Note, however, that this is not always the case, for example during the solar minimum of 2008–2009, when the quasi-dipolar nature of the HMF combines with inclination of the Earth’s orbit to preferentially produce near-Earth *T* sectors in the first half of the year and *A* sectors in the latter half.

### 3. Results

Taking the 2001 through 2006 datasets as a whole,  $\langle R_L \rangle = 25.1 \text{ day}^{-1}$  and  $\langle R_{TH} \rangle = 0.0210 \text{ day}^{-1}$ . Days associated

with *T* (*A*) sectors result in  $\langle R_L \rangle = 30.6 (18.5) \text{ day}^{-1}$  and  $\langle R_{TH} \rangle = 0.0240 (0.0175) \text{ day}^{-1}$ . Clearly *T* sectors are associated with substantially more (around 40–60%) UK thunderstorm activity than *A* sectors. These trends are also seen in the temporal correlations of lightning/thunder rates with HMF sector structure. Assigning *T*, *A* and undefined sectors values of  $-1, 1$  and  $0$ , respectively, we find a correlation coefficient of  $-0.0683 (-0.0724)$  with  $R_L (R_{TH})$ , with a sample size of  $N = 2134$ . While these correlations are small, as meteorological effects dominate the occurrence of thunder/lightning, the *p*-value is such that the null hypothesis (that the observed correlation occurred by chance) can be rejected above the 99.8%, or approximately the 3-sigma, confidence level.

In order to verify this is not simply the result of aliasing between the lightning seasonality and sector occurrence, we now consider the data relative to the seasonal mean. Seasonal mean variations in  $R_L$  and  $R_{TH}$ , shown as green lines in figures 1(b) and (c), are computed by taking the day-of-year average across the 6 years of data, then applying a 27 day running mean through these daily means. (Results are essentially unchanged for a wide range of smoothing time scales, from 5 to 50 day running means.) From these curves, we compute  $\Delta R_L$  and  $\Delta R_{TH}$ , daily deviations from the seasonal mean. Figures 2(b) and (c) show monthly means of  $\Delta R_L$  and  $\Delta R_{TH}$ , respectively, which are also clearly enhanced in *T* sectors and reduced in *A* sectors, particularly during the non-winter months.

The statistical significance of the difference between *T* and *A* means of  $\Delta R_L$  and  $\Delta R_{TH}$  is tested in two ways. Firstly, a Monte Carlo method is used. If there are  $N_T (N_A)$  days of *T* (*A*) sectors in a given subset of data (e.g., in JJA across the 6 years), 10 000 sets of  $N_T (N_A)$  daily values of  $\Delta R_L$  and  $\Delta R_{TH}$  are randomly selected from the same subset of data. These random samplings are used to create 10 000 *T* and *A* means and hence 10 000 random values of  $\langle \Delta R_L \rangle_T$  and  $\langle \Delta R_L \rangle_A$ . The null hypothesis (that the observed value of  $\langle \Delta R_L \rangle_T - \langle \Delta R_L \rangle_A$  occurred by chance sampling) can be rejected at a confidence level equal to the percentage of random values of  $\langle \Delta R_L \rangle_T - \langle \Delta R_L \rangle_A$  below that observed. The second method of significance testing is the Kolmogorov–Smirnov (*K–S*) test (e.g., [31]), which assesses the difference in the *T* and *A* cumulative distributions of  $\Delta R_L$  or  $\Delta R_{TH}$  and hence determines the probability at which the null hypothesis can be dismissed, that the *T* and *A* distributions are two sub-samples of the same underlying distribution.

Taken over the whole year,  $\Delta R_L (\Delta R_{TH})$  for *T* exceeds that for *A* such that the null hypothesis, that the means are the same within sampling uncertainty, can be rejected at the 99.8% (99.96%) confidence level using a Monte Carlo selection of the same data, and 98.8% (98.4%) level using the Kolmogorov–Smirnov test of the two distributions. These confidence levels are approximately at the 3 sigma level. Dividing the data into seasons,  $\langle \Delta R_L \rangle_T$  exceeds  $\langle \Delta R_L \rangle_A$  at the 99% confidence level for JJA and SON, while  $\langle \Delta R_{TH} \rangle_T$  exceeds  $\langle \Delta R_{TH} \rangle_A$  at the 99% confidence level for MAM and JJA. Figures 3(a) and (b) show that this is not the result of aliasing annual trends in thunderstorm activity with sector occurrence, as  $\langle \Delta R_L \rangle_T$  exceeds

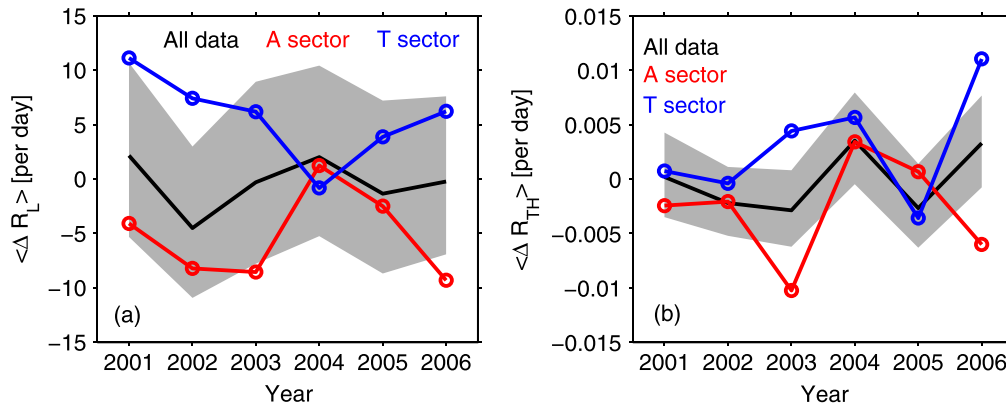


**Figure 3.** Annual means of (a) UK lightning rate relative to the seasonal mean,  $\Delta R_L$ , and (b) UK thunder day rate relative to the seasonal mean,  $\Delta R_{TH}$ , for all data (black), away (red) and toward (blue) heliospheric magnetic field sectors. Grey shaded areas show 90% of the variations over the whole dataset.

$\langle \Delta R_L \rangle_A$  (and  $\langle \Delta R_{TH} \rangle_T$  exceeds  $\langle \Delta R_{TH} \rangle_A$ ) for 5 of the 6 individual years of data, and  $\langle \Delta R_L \rangle_T$  and  $\langle \Delta R_L \rangle_A$  are found to be significantly different at the 90% confidence level for 2001, 2002, 2003 and 2006.

Ground-based neutron count rates serve as a proxy for the intensity of ionizing GCRs penetrating to the lower atmosphere. Applying the same sector analysis to data from Thule (Greenland), Newark (USA), McMurdo (Antarctica) and South Pole stations (e.g., [2]) for the 2001 through 2006 period does reveal a weak but significant trend for higher neutron counts in *A* than *T* sectors [28]. The expected solar cycle trends in GCR flux and the weak annual trends in *T* and *A* occurrence make this analysis problematic and it is not clear whether the neutron count rate trend is a result of changing GCR fluxes at the top of the atmosphere or changing magnetic access of energetic charged particles to the atmosphere. Most importantly for this study, the sector trend in GCR flux is only present in 3 of the 6 individual years and is only significant during JJA, meaning it is less prevalent than the lightning-HMF trends. Thus observed magnetic sector trends in UK thunderstorm activity cannot be explained by changes in near-Earth GCR flux alone.

#### 4. Discussion

Heliospheric magnetic sector structure is known to have a number of effects on magnetospheric and ionospheric structure [7] which may in turn affect local thunderstorm activity. (We note that magnetic sector control of the atmospheric electric circuit has also been proposed as the mechanism [3, 14] by which the HMF influences polar and mid-latitude surface pressure [13, 16, 29]). Figures 4(a) and (b) show how the HMF is essentially ‘superimposed’ on the Earth’s dipole, offsetting the magnetic axis from its nominal position. For *T* (*A*) sectors, the northern hemisphere ionospheric system is shifted a few degrees dusk-ward and anti-sunward (dawn-ward and sunward) [11]. Figures 4(c) and (d) show that the net effect is *A* sectors increase ionospheric

potential at dawn, while *T* sectors decrease ionospheric potential at dusk [10]. At the (nominally sub-auroral) geomagnetic latitude of the UK, this is likely to be a small effect, of order 10% of the total ionospheric potential relative to the ground [23]. Shifting the magnetosphere will also change the atmospheric foot point at which various energetic charged particle populations may precipitate down into the atmosphere, particularly ring current particles, which approximately track the outer boundary of the zero ionospheric potential line. Figure 4 is sketched such that *T* sectors result in UK latitudes encountering ring current particles for a much greater fraction of the day than *A* sectors, particularly in the post-noon and dusk sectors, when most thunderstorm activity occurs. In reality, however, the position of ionospheric features will be highly sensitive to a range of effects, particularly the size of the ionospheric polar cap, geomagnetic and geographic latitude, longitude and local time, as well as seasonal trends in the HMF-magnetosphere connectivity. This complexity may, in part, explain the opposing decadal [21, 27] and short-term [5, 26] responses observed in solar modulation of lightning. Preliminary analysis of global Met Office land surface weather records suggests a very complex response of lightning to HMF sector with geographic location, though the suitability of these proxy data for thunderstorm activity has still to be established via comparison with local radio networks and true thunder day records, and hence those data are not discussed further here.

Of course, it is necessary to quantify local changes in ionospheric potential and energetic charged particle flux with sector structure, in order to determine if they are of sufficient amplitude to explain the observed trends in thunderstorm activity. There are, however, qualitative arguments for both ionospheric potential and particle fluxes influencing lightning through the local atmospheric electric circuit: reduced ionospheric potential would extend down into the sub-ionospheric atmosphere [1], whereas increased charged particle flux at high altitudes would enhance atmospheric conductivity in the sub-ionospheric gap, both effects influencing cloud-to-

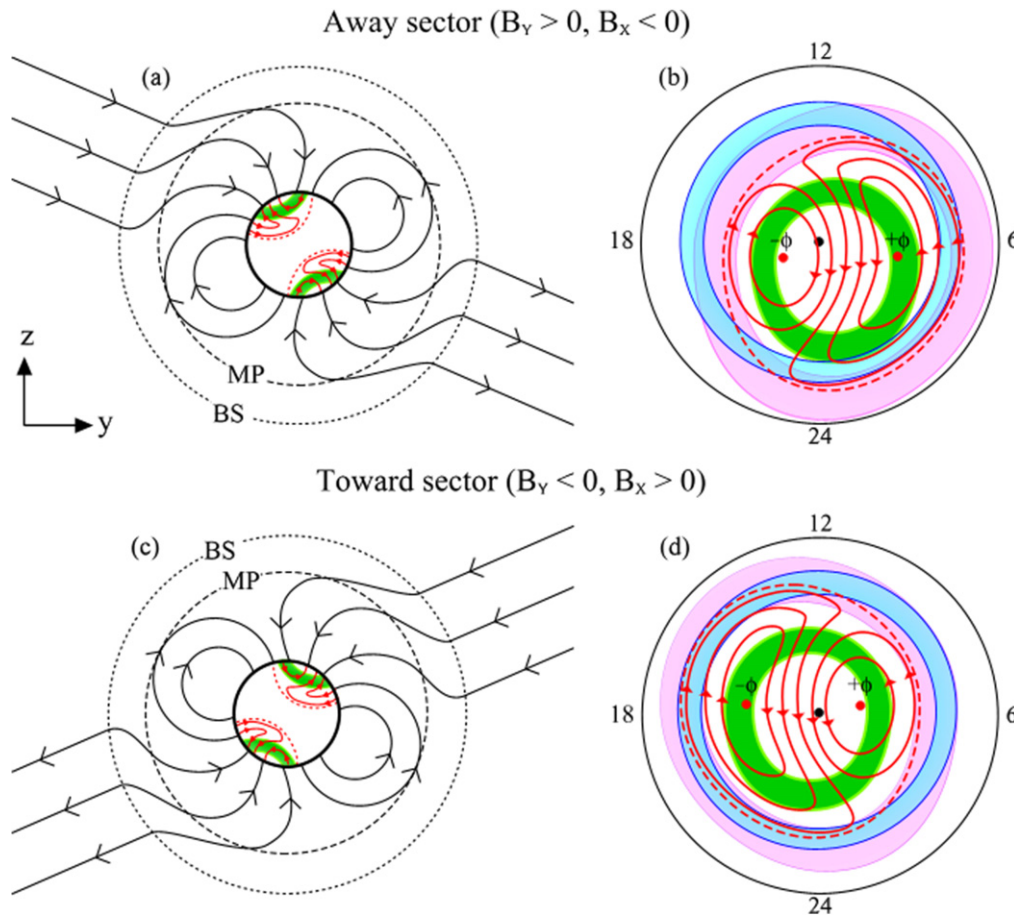


**Figure 4.** Sketches of magnetospheric and ionospheric variations resulting from HMF sector structure (not to scale). Negative HMF  $B_z$  is shown. Left: dawn-dusk meridian, viewed from the Sun. Closed magnetospheric loops are confined within the magnetopause (MP), while the HMF is unperturbed outside the bow shock (BS). The auroral oval is shown in green, ionospheric convection streamlines in red. The outer boundary of zero ionospheric potential is shown as a dashed red line. Right: the northern hemisphere ionosphere in magnetic coordinates, with local noon at the top. The magnetic pole is shown as a black dot. The position of the UK is shown as a blue band, while the ionospheric foot point of the ring current is shaded pink.

ionosphere current which allows thunder clouds to discharge via sprites and blue jets (e.g., [20] and references therein). Enhanced conductivity down to cumulonimbus cloud top height [17] could also enhance weaker intra-cloud discharge, which is both harder to detect with the ATD network and less audible. It is not presently clear, however, how cloud-to-ground lightning rates respond to these effects. In addition to atmospheric electric circuit effects, sufficiently energetic charged particles may be able to provide narrow ionization channels that trigger cloud-to-ionosphere, intra-cloud or CG discharges, which may or may not be important for the observed trends. Differentiating between the proposed mechanisms will require full characterization of the global relation of thunderstorm activity to HMF, which will require careful analysis of long-term global lightning networks and thunder day records. It may also be necessary to comprehensively characterize the vertical charged particle distribution and ionospheric potential, at a range of geomagnetic latitudes and longitudes, and under differing HMF regimes. This would require coordinated observational campaigns beyond those currently performed.

### 5. Summary

The large-scale HMF consists of sectors of toward (*T*) and away (*A*) polarity, which are known to skew the Earth's magnetic field in opposing manners. In this study, UK lightning and thunder rates are shown to be significantly different when the Earth is embedded in *T* or *A* sectors, with 40–60% more thunderstorm activity in *T* sectors than *A* sectors. This result persists even when the strong seasonal variation in thunderstorm activity is removed. Comparing with global neutron monitor measurements, this does not seem to be solely the result of changes in the global top-of-the-atmosphere energetic charged particle flux, which is the mechanism by which previous studies have suggested solar modulation of lightning. Instead, we propose a redistribution of lightning, rather than a global change in the lightning rate. The *T/A*-sector skewing of the Earth's magnetic field relative to a fixed geographic position will change both the local ionospheric potential and the atmospheric footprints of various energetic charged particle populations. This, in turn, may change the discharge processes in electrified storm clouds, though the mechanisms have yet to be established.

## Acknowledgements

We would like to thank the UK Met Office for use of data from their ATD network and observing stations which were made available via the NCAS British Atmospheric Data Centre (BADC) at <http://badc.nerc.ac.uk>. Thunder day data were obtained from the Met Office Integrated Data Archiving System (MIDAS) land and marine surface stations, made available by BADC. We are grateful to the Space Physics Data Facility (SPDF) of NASA's Goddard Space Flight Centre for combining the data into the OMNI 2 dataset which was obtained via the GSFC/SPDF OMNIWeb interface at <http://omniweb.gsfc.nasa.gov>. We also thank the Bartol Research Institute of the University of Delaware for the neutron monitor data from McMurdo, which is supported by NSF grant ATM-0527878.

## References

- [1] Bering E, Engebretson M, Holzworth R, Kadokura A, Kokorowski M, Reddell B, Posch J and Yamagishi H 2009 Simultaneous observations of Pc 1 micropulsation activity and stratospheric electrodynamic perturbations on 27 January 2003 *Adv. Space Res.* **43** 802–18
- [2] Bieber J W, Evenson P, Dröge W, Pyle R, Ruffolo D, Rujiwarodom M, Tooprakai P and Khumlumlert T 2004 Spaceship earth observations of the easter 2001 solar particle event *Astrophys. J. Lett.* **601** 103–6
- [3] Burns G B, Tinsley B A, French W J R, Troshichev O A and Frank-Kamenetsky A V 2008 Atmospheric circuit influences on ground-level pressure in the Antarctic and Arctic *J. Geophys. Res.* **113** 15112
- [4] Carey L D and Rutledge S A 1996 A multiparameter radar case study of the microphysical and kinematic evolution of a lightning producing storm *Meteorol. Atmos. Phys.* **59** 33–64
- [5] Christensen J H and Christensen O B 2003 Climate modelling: severe summertime flooding in Europe *Nature* **421** 805–6
- [6] Chronis T G 2009 Investigating possible links between incoming cosmic ray fluxes and lightning activity over the united states *J. Clim.* **22** 5748
- [7] Cowley S W H, Morelli J P and Lockwood M 1991 Dependence of convective flows and particle precipitation in the high-latitude dayside ionosphere on the X and Y components of the interplanetary magnetic field *J. Geophys. Res.* **96** 5557–64
- [8] Deierling W, Petersen W A, Latham J, Ellis S and Christian H J 2008 The relationship between lightning activity and ice fluxes in thunderstorms *J. Geophys. Res.* **113** 15210
- [9] Giles Harrison R and Usoskin I 2010 Solar modulation in surface atmospheric electricity *J. Atmos. Sol.-Terr. Phys.* **72** 176–82
- [10] Greenwald R A, Baker K B, Ruohoniemi J M, Dudeney J R, Pinnock M, Mattin N, Leonard J M and Lepping R P 1990 Simultaneous conjugate observations of dynamic variations in high-latitude dayside convection due to changes in IMF by *J. Geophys. Res.* **95** 8057–72
- [11] Holzworth R H and Meng C-I 1984 Auroral boundary variations and the interplanetary magnetic field *Planet. Space Sci.* **32** 25–29
- [12] King J H and Papitashvili N E 2005 Solar wind spatial scales in and comparisons of hourly wind and ACE plasma and magnetic field data *J. Geophys. Res.* **110** A02104
- [13] Lam M M, Chisham G and Freeman M P 2013 The interplanetary magnetic field influences mid-latitude surface atmospheric pressure *Environ. Res. Lett.* **8** 045001
- [14] Lam M M, Chisham G and Freeman M P 2014 Solar-wind-driven geopotential height anomalies originate in the Antarctic lower troposphere *Geophys. Res. Lett.* in press doi:10.1002/2014GL061421
- [15] Lee A C L 1989 Ground truth confirmation and theoretical limits of an experimental VLF arrival time difference lightning flash locating system *Q. J. R. Meteorol. Soc.* **115** 1147–66
- [16] Mansurov S M, Mansurova L G, Mansurov G S, Mikhnevich V V and Visotskii A M 1974 North–south asymmetry of geomagnetic and tropospheric events *J. Atmos. Terr. Phys.* **36** 1957–62
- [17] Nicoll K A and Harrison R G 2014 Detection of lower tropospheric responses to solar energetic particles at midlatitudes *Phys. Res. Lett.* **112** 225001
- [18] Owens M J and Forsyth R J 2013 The heliospheric magnetic field *Living Rev. Sol. Phys.* **10** 5
- [19] Parker E N 1958 Dynamics of the interplanetary gas and magnetic fields *Astrophys. J.* **128** 664–76
- [20] Pasko V P, Stanley M A, Mathews J D, Inan U S and Wood T G 2002 Electrical discharge from a thundercloud top to the lower ionosphere *Nature* **416** 152–4
- [21] Pinto Neto O, Pinto I R C A and Pinto O 2013 The relationship between thunderstorm and solar activity for Brazil from 1951 to 2009 *J. Atmos. Sol.-Terr. Phys.* **98** 12–21
- [22] Roussel-Dupré R, Colman J J, Symbalysty E, Sentman D and Pasko V P 2008 Physical processes related to discharges in planetary atmospheres *Space Sci. Rev.* **137** 51–82
- [23] Rycroft M J, Israelsson S and Price C 2000 The global atmospheric electric circuit, solar activity and climate change *J. Atmos. Sol.-Terr. Phys.* **62** 1563–76
- [24] Saunders C P R, Bax-Norman H, Emersic C, Avila E E and Castellano N E 2006 Laboratory studies of the effect of cloud conditions on graupel/crystal charge transfer in thunderstorm electrification *Q. J. R. Meteorol. Soc.* **132** 2653–73
- [25] Schlegel K, Diendorfer G, Thern S and Schmidt M 2001 Thunderstorms, lightning and solar activity-middle Europe *J. Atmos. Sol.-Terr. Phys.* **63** 1705–13
- [26] Scott C J, Harrison R G, Owens M J, Lockwood M and Barnard L 2014 Evidence for solar wind modulation of lightning *Environ. Res. Lett.* **9** 055004
- [27] Stringfellow M F 1974 Lightning incidence in Britain and the solar cycle *Nature* **249** 332–3
- [28] Thomas S R, Owens M J, Lockwood M and Scott C J 2014 Galactic cosmic ray modulation near the heliospheric current sheet *Sol. Phys.* **289** 2653–68
- [29] Tinsley B A and Heelis R A 1993 Correlations of atmospheric dynamics with solar activity evidence for a connection via the solar wind, atmospheric electricity, and cloud microphysics *J. Geophys. Res.* **98** 10375–84
- [30] Wilkinson Jonathan M and Jorge Bornemann F 2014 A lightning forecast for the London 2012 Olympics opening ceremony *Weather* **69** 16–19
- [31] York D, Evensen N M, Lo M, Nez M, De J S and Delgado B 2004 Unified equations for the slope, intercept, and standard errors of the best straight line *Am. J. Phys.* **72** 367